Allee pits in metapopulations: critical dispersal rates for connectivity to be beneficial

Carolin Grumbach[1*] and Frank M. Hilker[1]

[1]Institute of Mathematics and Institute of Environmental Systems Research, Osnabrück University, Barbarastraße 12, Osnabrück, 49076, Germany.

*Corresponding author(s). E-mail(s): carolin.grumbach@uni-osnabrueck.de;
Contributing authors: frank.hilker@uni-osnabrueck.de;

Abstract

Habitat fragmentation divides populations into smaller subpopulations. At the same time, the Allee effect reduces the growth and thereby the viability of small populations. Hence, habitat fragmentation and the Allee effect can synergistically amplify negative impacts on spatially distributed populations. To support endangered populations, management and conservation strategies aim to improve connectivity between subpopulations by creating corridors and stepping stones, for instance. This study investigates how enhanced connectivity (strength of connections between subpopulations in terms of dispersal rate) influences a fragmented population subject to the Allee effect. Using a generic two-patch discrete–time model with a positively density-dependent growth function, we study the impact of connectivity on the asymptotic total population size through simulations. Due to the Allee effect, low connectivity can lead to a decline in the asymptotic total population size, which we call the Allee pit. However, increased connectivity facilitates the rescue effect, wherein a persistent subpopulation in one patch can save an extinction-prone subpopulation in another patch. We find that for connectivity to benefit the asymptotic total population size, dispersal must be sufficiently large to push the smaller subpopulation above its Allee threshold. If dispersal is below this critical dispersal rate, there remains a detrimental effect on the asymptotic total populations size. Therefore, this study implies that conservation strategies should not only aim to increase connectivity in fragmented populations subject to Allee effects but also ensure that the critical dispersal rate is surpassed.

Keywords: spatial fragmentation, two-patch model, connectivity, Allee effect, total population size, rescue effect

1 Introduction

Fragmentation of land and sea due to human activities stands as a paramount challenge in biodiversity conservation efforts, as highlighted by the Intergovernmental Science-Policy Platform on Biodiversity and Ecosystem Services (IPBES, 2019). In contrast to the negative density-dependence arising from competition, positive density-dependence — the well known Allee effect — puts small populations under pressure and makes them more extinction prone (Courchamp et al, 2008). As habitat fragmentation splits up populations in smaller subpopulations, the Allee effect can reinforce negative consequences of fragmentation.

Mechanisms like mate-finding difficulties or predation can cause an Allee effect (Dennis, 1989; Schreiber, 2003; Gascoigne et al, 2009; Kramer et al, 2009). For instance, the mate-finding Allee effect describes a decrease of mating opportunities with decreasing population densities. Especially for individuals of a small population this mating difficulty and lacking cooperation opportunities are a disadvantage that can make a population not viable. The Allee effect is therefore of high relevance for extinction research (Courchamp et al, 1999). If a subpopulation with an Allee effect is connected to other patches by dispersal, immigrants from another patch might support the local population on the one hand. On the other hand, the immigrants may be exposed to an increased risk of extinction due to the Allee effect. This could lead to a total net loss of individuals in the metapopulation and even increase its vulnerability. Consequently, the Allee effect can make it more likely to reinforce negative consequences of fragmentation. Increasing dispersal in such a situation can intensify this negative effect on the total population.

This is a fundamental issue because many conservation efforts aim at increasing connectivity to enhance reproductive success and potentially reducing the risk of extinction (Tewksbury et al, 2002; Fahrig, 2002), and promoting dispersal, e.g., via corridors over highways, stepping stones, or flowering edges of cultivated land (Turner et al, 2001; Soanes et al, 2024). While such measures are often perceived as 'beneficial', it is long recognized that they can come with disadvantages caused by several factors (Simberloff and Cox, 1987; Haddad et al, 2014). For example, diseases, natural enemies, invasive species and fire can spread more easily between patches when they are more tightly coupled. Predators can adapt behaviorally and wait around corridors for their prey, and connectivity can synchronize population dynamics and increase the chance of extinction (Matter, 2001).

These insights naturally raise the question to which degree the interplay between enhanced connectivity and positive density dependence benefits or endangers a population in a fragmented habitat. Here, we aim to investigate the influence of the relationship between increased dispersal and the Allee effect on the asymptotic total population size.

This seems to have not been done so far, which is somewhat surprising as the Allee effect has been extensively studied in patchy environments. In a discrete-time model Vortkamp et al (2020) analyzed the effect of increased connectivity and a strong Allee effect on population persistence and stability in a two-patch model with the Ricker growth function, and in a continuous-time model Gyllenberg et al (1999) studied the joint effect of symmetric dispersal and the Allee effect on the heterogeneity of population densities. Amarasekare (1998) studied dispersal and a strong Allee effect in two patches and found that if one subpopulation size falls below the Allee threshold the patch can be rescued by immigrants from the other patch that is above the threshold (referred to as the *rescue effect*; also explored in e.g., Brown and Kodric-Brown, 1977; Gotelli, 1991; Kang, 2013; Van Schmidt and Beissinger, 2020). Wang (2016) investigated the joint effect of dispersal and a strong Allee effect as well and stated that there is an optimal dispersal rate at which migration to the 'better' patch is beneficial for each individual, and above which migration is harmful to the whole species. Moreover, the Allee effect was studied in two-patch models with respect to stability (Pal and Samanta, 2018; Saha and Samanta, 2019; Chen et al, 2022), invasion and persistence (Maciel and Lutscher, 2015), synchrony (Kang and Armbruster, 2011), and within more general patchy environments (Ferdy and Molofsky, 2002; Sato, 2009; Sun, 2016; Cronin et al, 2020), for example.

We tackle our research aim through simulations and numerical exploration. Here, we consider a discrete-time two-patch model that represents two subpopulations and we assume Beverton–Holt growth with an Allee effect. Focusing on spatial heterogeneity, we assume different intrinsic growth rates and carrying capacities for the two subpopulations.

Fahrig (2017) found in a literature review that fragmentation per se, i.e., the division of habitat into smaller patches without reducing the total habitat amount, has been reported to have more positive than negative effects (in the sense of affecting population occurrence, abundance, species richness, or other ecological response variables). This initiated a debate about the ecological consequences of habitat fragmentation (Fletcher Jr et al, 2018; Fahrig et al, 2019; Miller-Rushing et al, 2019). More recently, it has been shown that spatial heterogeneity can have detrimental effects as well when certain relationships between intrinsic growth and the carrying capacity (i.e., r–K relationships) are fulfilled (DeAngelis and Zhang, 2014; Arditi et al, 2015; Zhang et al, 2017; DeAngelis et al, 2020; Vortkamp et al, 2022; Grumbach et al, 2023).

We build upon the classification of the effect of dispersal on the asymptotic total population size into four qualitatively different so-called *response scenarios* (Grumbach et al, 2023), see Fig. 1. When two connected patches achieve an asymptotic total population size greater (lesser) than the combined carrying capacities of the individual patches for all dispersal rate values, this outcome is termed a *beneficial* (*detrimental*, respectively) effect of dispersal (and therefore of connectivity). The sum of the two carrying capacities is the asymptotic total population size in the absence of dispersal and therefore serves as the reference value for isolation in comparison with connectivity.

In this paper we will show that the inclusion of the Allee effect can introduce a critical dispersal rate below which dispersal has a detrimental effect while larger dispersal rates can have a beneficial effect on the asymptotic total population size due

to the rescue effect. The detrimental dip for small dispersal rates is later introduced as the *Allee pit*. We therefore detect and classify so far unknown response scenarios including the Allee pit, which we propose to call *pit response scenarios*. We also provide a mechanistic explanation of the new pit response scenarios and a biological interpretation of the emerging rescue effect across various parameter ranges.

2 Setting the stage

2.1 Model description

The simplest setting for a fragmented population can be modeled by a two-patch system. There are two subpopulations A and B, and their population sizes are denoted as $N_{\mathrm{A},t}$ and $N_{\mathrm{B},t}$ at time step $t \in \mathbb{N}$ respectively. The asymptotic total population size is the sum of the two asymptotic subpopulation sizes denoted by $N_{\mathrm{tot}} = N_{\mathrm{A}}^* + N_{\mathrm{B}}^*$. The two subpopulations are connected by dispersal with dispersal rate δ, which for simplicity is assumed to be symmetric in both patches, i.e., $\delta_{\mathrm{A}} = \delta_{\mathrm{B}} = \delta$. We assume the dispersal rate to be $\delta \leq 0.5$, i.e., the largest dispersal value leads to perfect mixing of the two subpopulations.

We consider the two-dimensional discrete-time model where reproduction $f_i^\theta(N_{i,t})$ in the individual patches $i = \mathrm{A}, \mathrm{B}$ depends on the Allee effect strength $\theta \in \mathbb{R}^+$ and is taking place before dispersal:

$$\begin{aligned} N_{\mathrm{A},t+1} &= (1-\delta) f_{\mathrm{A}}^\theta(N_{\mathrm{A},t}) + \delta f_{\mathrm{B}}^\theta(N_{\mathrm{B},t}), \\ N_{\mathrm{B},t+1} &= (1-\delta) f_{\mathrm{B}}^\theta(N_{\mathrm{B},t}) + \delta f_{\mathrm{A}}^\theta(N_{\mathrm{A},t}). \end{aligned} \tag{1}$$

The growth functions read

$$f_i^\theta(N_{i,t}) = \frac{r_i N_{i,t}}{1 + \xi_i N_{i,t}} \cdot \frac{N_{i,t}}{N_{i,t} + \theta}, \quad i = \mathrm{A}, \mathrm{B}, \tag{2}$$

which consist of two parts. The first factor describes Beverton–Holt growth and the second factor describes the mate-finding Allee effect (Courchamp et al, 2008; Boukal and Berec, 2009) with Allee strength θ, which describes the difficulty of finding mating partners. The parameters $r_i \in \mathbb{R}^+$ are the intrinsic growth rates and $\xi_i \in \mathbb{R}^+$ are the intraspecific competition strengths. From now on, when we use i in the subscript of subpopulation sizes and parameters, we always mean $i = \mathrm{A}, \mathrm{B}$.

In the absence of the Allee effect ($\theta = 0$), the growth dynamics coincide with the Beverton–Holt dynamics. In terms of the intraspecific competition strengths, the carrying capacitiy of the Beverton–Holt function (i.e., the positive fixed point of f_i^0) can be expressed by $K_i^{\mathrm{BH}} = \frac{r_i - 1}{\xi_i}$. We proceed under the assumption that $K_{\mathrm{A}}^{\mathrm{BH}} \leq K_{\mathrm{B}}^{\mathrm{BH}}$, allowing us to refer to patch A as 'the smaller patch' and patch B as 'the larger patch' ($K_{\mathrm{A}}^{\mathrm{BH}} \geq K_{\mathrm{B}}^{\mathrm{BH}}$ would symmetrically yield identical outcomes). If $r_i > 1$, both patches approach their carrying capacity when being isolated. Contrarily, if $r_i < 1$ each of the subpopulations goes extinct in isolation. Therefore, in the absence of the Allee effect, $r_i = 1$ is the threshold between long-term persistence and extinction. In presence of the

Allee effect this threshold increases, i.e., with increasing Allee strength the population growth rate needs to increase such that the population persists.

The Allee strength θ is assumed to be symmetric in both patches (suppose that both subpopulations are biologically similar and therefore suffer the same mate-finding difficulties in case of low density). It influences the Beverton–Holt growth dynamics to have a positive density-dependence. For $\theta > 0$, a strong demographic Allee effect is induced, i.e., there is an Allee threshold below which the per-capita growth rate is smaller than one and the population goes extinct.

2.2 Isolated patches with Allee effect

For a single population (i.e., both subpopulations in isolation) with growth dynamics (2) and an Allee effect strength $\theta > 0$, there are up to three equilibria. The two stable equilibria are zero and the carrying capacity K_A or K_B. They are separated by an unstable equilibrium which is the Allee threshold T_A or T_B (cf. Kang (2015) for a more general model). Population sizes below the Allee threshold decrease to extinction, while population sizes above the Allee threshold grow to the carrying capacity. The two nontrivial equilibria read

$$\begin{aligned} K_i &= \frac{\alpha + \sqrt{\alpha^2 - \beta}}{2(r_i - 1)}, \\ T_i &= \frac{\alpha - \sqrt{\alpha^2 - \beta}}{2(r_i - 1)}, \end{aligned} \tag{3}$$

with

$$\begin{aligned} \alpha &= (r_i - 1)(K_i^{\mathrm{BH}} - \theta), \\ \beta &= 4K_i^{\mathrm{BH}}\theta(r_i - 1). \end{aligned}$$

The carrying capacity and the Allee threshold exist if and only if the radicand of the square root is non-negative and the denominator is non-zero, i.e., if $r_i \neq 1$. The radicands of K_i and T_i coincide and therefore vanish for the same value of θ, which is

$$\theta_{\mathrm{c},i} = K_i^{\mathrm{BH}} \frac{\sqrt{r_i} - 1}{\sqrt{r_i} + 1}. \tag{4}$$

If θ is greater than this critical value $\theta_{\mathrm{c},i}$, the radicand is negative and therefore the nontrivial equilibria do not exist. In this case, the population goes extinct for all initial conditions.

In the absence of the Allee effect (i.e., for $\theta = 0$), the equilibrium subpopulation sizes K_i coincide with the respective carrying capacity parameters K_i^{BH} in the Beverton–Holt dynamics, provided $r_i > 1$. For increased Allee strength the asymptotic subpopulation sizes K_i decrease (note that the carrying capacity is approached only for initial conditions within this equilibrium's basin of attraction).

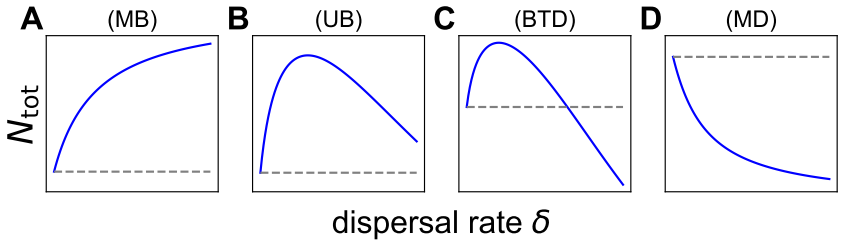

Fig. 1 The asymptotic total population size N_{tot} of two coupled patches without Allee effect ($\theta = 0$) in terms of the dispersal rate δ for four different response scenarios. A: (MB) monotonically beneficial, B: (UB) unimodally beneficial, C: (BTD) beneficial turning detrimental and D: (MD) monotonically detrimental. The dashed horizontal line corresponds to the sum of the two carrying capacities, $K_{\text{A}}^{\text{BH}} + K_{\text{B}}^{\text{BH}}$, which is the asymptotic total population in the absence of dispersal. It serves as the reference value.

2.3 Connected patches without Allee effect

Before investigating the dynamics of the coupled model (1)-(2), we briefly outline the impact of dispersal on the asymptotic total population size in the case $\theta = 0$, which has been analyzed by Grumbach et al (2023). They give explicit parameter conditions and a biological interpretation for four qualitatively different response scenarios (see Fig. 1). In case of no dispersal the total population size N_{tot} approaches the sum of the two carrying capacities $K_{\text{A}}^{\text{BH}} + K_{\text{B}}^{\text{BH}}$, which is shown in a dashed horizontal reference line in Fig. 1. The sum of the two carrying capacities serves as the reference value to designate beneficial and detrimental effects of increasing dispersal rates on the asymptotic total population. The four response scenarios can be briefly characterized as follows:

(MB) In the *monotonically beneficial* response scenario the asymptotic total population size increases monotonically with increasing dispersal (see Fig. 1A).

(UB) The scenario where increasing dispersal is consistently beneficial for the asymptotic total population size, albeit with decreasing benefit for high dispersal rates, is termed the "unimodally beneficial" response scenario (see Fig. 1B).

(BTD) We speak of the *beneficial turning detrimental* response scenario if increasing dispersal has a beneficial effect on the asymptotic total population size for small dispersal, but a detrimental effect for larger dispersal (see Fig. 1C).

(MD) If the asymptotic total population size monotonically decreases with increasing dispersal the response scenario is called *monotonically detrimental* (see Fig. 1D).

Mechanistically the scenarios differ mainly due to the patches' spatial heterogeneity (depending on r_i and K_i^{BH}). In case of overcrowding in one of the patches (i.e., large growth rate and large competition) it is beneficial for the asymptotic total population size if many individuals disperse to the other patch in which they are subject to more relaxed conditions with less competition. In that case the less crowded patch

can absorb individuals like a sponge. By contrast, in case of a net flow from relaxed conditions into a patch which is already overcrowded, the pressure on the entire population is even strengthened, which leads to a detrimental effect on the asymptotic total population size. The analytic parameter ranges for these four response scenarios were published in Grumbach et al (2023). Their results build on Franco and Ruiz-Herrera (2015), Arditi et al (2015) and Gao and Lou (2022).

2.4 Connected patches with Allee effect

We now look at the dynamics of two connected patches with the Allee effect ($\theta > 0$) as introduced in Eq. (1). In Section 2.1, we already pointed out that in isolation each subpopulation can have up to three equilibria, two of which are stable: the carrying capacity and population extinction. When connecting the two subpopulations, there are up to nine equilibria with quadristability.

Figure 2 shows the nullclines of the two subpopulations in the phase plane (cf. Amarasekare, 1998). In Figure 2A we see that for $\delta = 0$ the coupled system has nine equilibria, which are all combinations of $\{0,\ T_\mathrm{A},\ K_\mathrm{A}\}$ and $\{0,\ T_\mathrm{B},\ K_\mathrm{B}\}$. The equilibrium subpopulation sizes are independent of the other subpopulation's size (as they are not connected). The four stable equilibria of the coupled system are $(K_\mathrm{A}, K_\mathrm{B})$, $(K_\mathrm{A}, 0)$, $(0, K_\mathrm{B})$, and $(0, 0)$. There is only one stable equilibrium of the coupled system at which both subpopulations persist. In the following, we will refer to the coexistence equilibrium $(K_\mathrm{A}, K_\mathrm{B})$ as E_Coex.

For increased δ we see in Fig. 2B that there is still quadristability. The increased dispersal rate induces that there are three stable equilibria at which both subpopulations survive. At the two additional coexistence equilibria (referred to as E_lowA and E_lowB for N_A^* and N_B^* close to zero, respectively), connectivity enables the larger subpopulation to rescue the smaller subpopulation, which would go extinct in the absence of dispersal. Even though the two additional coexistence equilibria E_lowA and E_lowB are stable, they have a high sensitivity to external variations as one of the subpopulation sizes is close to zero.

Figure 2C and 2E show the nullclines for slight variations of the parameters r_A and K_A^BH. These parameter variations change the system to have seven equilibria (three of which are stable) in Fig. 2C and five equilibria (two of which are stable) in Fig. 2E. We see that the coupled system (for $\delta > 0$) is highly sensitive to parameter changes. An increased dispersal rate can change the system's dynamics and stable states in different ways. In Fig. 2D and 2F we see the same parameter settings as in Fig. 2C and 2E, respectively, but with an increased dispersal rate. In Fig. 2D the total number of equilibria differs compared to Fig. 2C while the characteristics of the stable states are unchanged. In Fig. 2F the coexistence equilibrium E_lowA disappears while E_Coex appears in comparison to Fig. 2E. The total number of equilibria is unchanged.

In our following results we choose an initial condition $N_{\mathrm{A},0} = N_{\mathrm{B},0} = 1$, that always makes the system approach the stable equilibrium $E_\mathrm{Coex} = (K_\mathrm{A}, K_\mathrm{B})$ if it exists. As Fig. 2E illustrates, there are settings in which the equilibrium E_Coex does not exist. In these situations our chosen initial condition approaches either one of the coexistence equilibria E_lowA and E_lowB or $(0, 0)$, depending on the parameter setting.

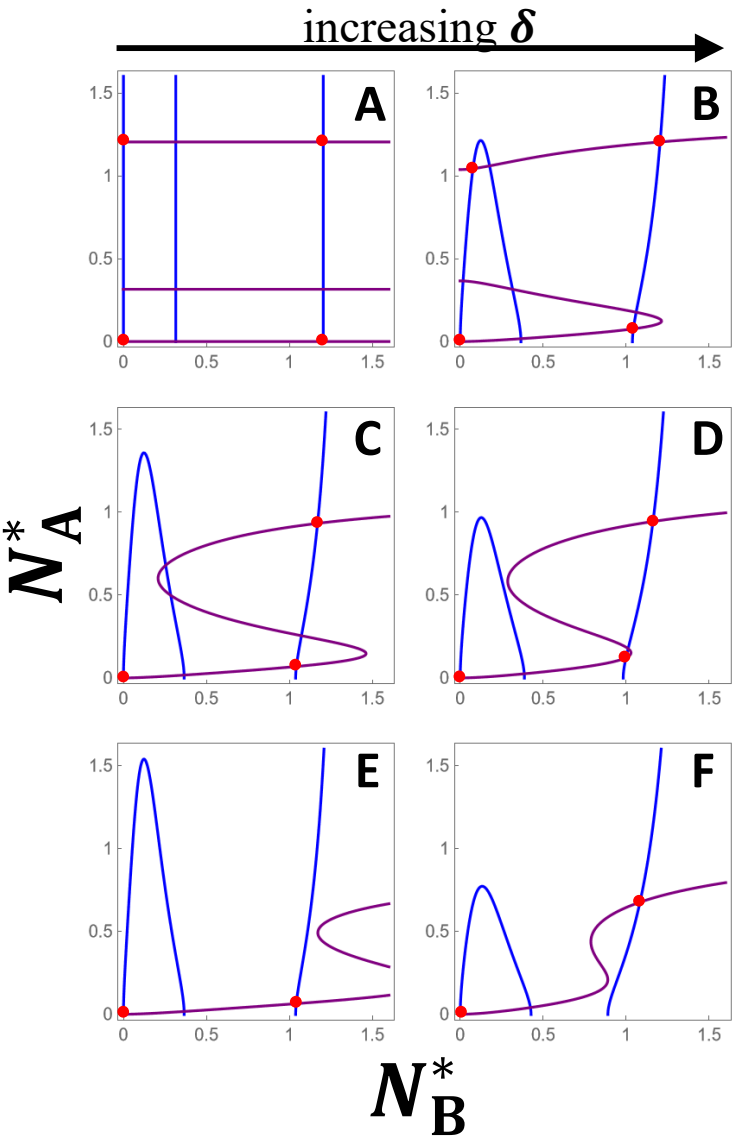

Fig. 2 The equilibria and their stability in the phase plane. The purple lines correspond to the nullclines of subpopulation A and the blue lines correspond to the nullclines of subpopulation B. The intersections of the two lines are the equilibrium states of the coupled system. The red points mark the stable equilibria. In panel A the patches are isolated, in panels B–E the patches are connected. Parameters: $r_{\mathrm{B}} = 2.9$, $K_{\mathrm{B}}^{\mathrm{BH}} = 1.9$ and $\theta = 0.38$. Additionally, we chose in A and D: $r_{\mathrm{A}} = 2.9$, $K_{\mathrm{A}}^{\mathrm{BH}} = 1.9$ with $\delta = 0$ in A and $\delta = 0.04$ in D; B and E: $r_{\mathrm{A}} = 2.69$, $K_{\mathrm{A}}^{\mathrm{BH}} = 1.69$ with $\delta = 0.04$ in B and $\delta = 0.052$ in E; C and F: $r_{\mathrm{A}} = 2.49$, $K_{\mathrm{A}}^{\mathrm{BH}} = 1.49$ with $\delta = 0.04$ in C and $\delta = 0.07$ in F.

3 Results

3.1 Rescue effects and Allee pits

We now focus on the question to which degree the interplay between enhanced connectivity and the Allee effect benefits or diminishes the total population. Figure 3 shows the asymptotic subpopulation sizes as functions of the Allee strength and the asymptotic total population size as a function of the dispersal rate. First, we consider the effect of increasing Allee effect strength θ.

Figure 3A shows the two asymptotic subpopulation sizes in isolation. As explained in Sect. 2.4, for the chosen initial condition $(1, 1)$ the system approaches the stable equilibrium $E_{\mathrm{Coex}} = (K_{\mathrm{A}}, K_{\mathrm{B}})$ for all Allee strengths smaller than each of the critical values $\theta_{\mathrm{c},i}$, depicted in Fig. 3A. The critical Allee strength $\theta_{\mathrm{c},i}$ is the bifurcation point of the underlying saddle-node bifurcation for each subpopulation. As the Allee strength increases, so does the Allee threshold, causing more initial conditions to approach zero. For Allee strengths in between both critical Allee strength, i.e., $\theta_{\mathrm{c,A}} < \theta < \theta_{\mathrm{c,B}}$, subpopulation A is extinct for all initial conditions, while subpopulation B still approaches its carrying capacity (as the initial condition's value for subpopulation B is sufficiently large in patch B). Beyond the critical Allee strength $\theta_{\mathrm{c,B}}$, global extinction occurs for all initial conditions.

Increased connectivity facilitates rescue mechanisms which can enable the smaller patch to persist even for Allee strengths beyond $\theta_{0,\mathrm{A}}$ where it would go extinct in isolation. Figure 3B–3D show the rescue effect in different intensities depending on the degree of connectivity, i.e., the dispersal value δ.

- In Fig. 3B we see that already very little connectivity ($\delta = 0.015$) enables the larger patch B to help patch A to persist beyond the critical Allee strengths $\theta_{\mathrm{c,A}}$, i.e., the left red vertical line. The rescue effect is not strong enough to prevent patch A from dying out for all Allee strengths but it delays the extinction (in terms of greater Allee strength).
- A little increase in connectivity, as shown in Fig. 3C ($\delta = 0.075$), can prevent patch A from dying out before patch B dies out. Moreover, in this setting the subpopulation in patch A shrinks close to zero with increasing Allee strength and is therefore already at high risk of stochastic extinction for intermediate Allee strengths. Here, we remind the choice of the initial condition such that the equilibrium E_{Coex} is approached (explained in Sect. 2.4). Even for this choice, the Allee effect can put the subpopulations and therefore the total population under incresed risk of extinction.
- For further increased connectivity, as shown in Fig. 3D ($\delta = 0.17$), the rescue effect prevents patch A from going extinct before patch B without high risk of stochastic extinction. The subpopulation sizes N_{A}^* and N_{B}^* come closer to each other while the Allee strength beyond which both subpopulations go extinct declines.

For Allee strengths just above $\theta_{\mathrm{c,A}}$ the total population takes big benefit from increasing connectivity and the resulting rescue effect. But the rescue effect also has its drawback. The larger the impact of the rescue effect on the smaller subpopulation, the lower the Allee strengths above which complete extinction of the total population occurs.

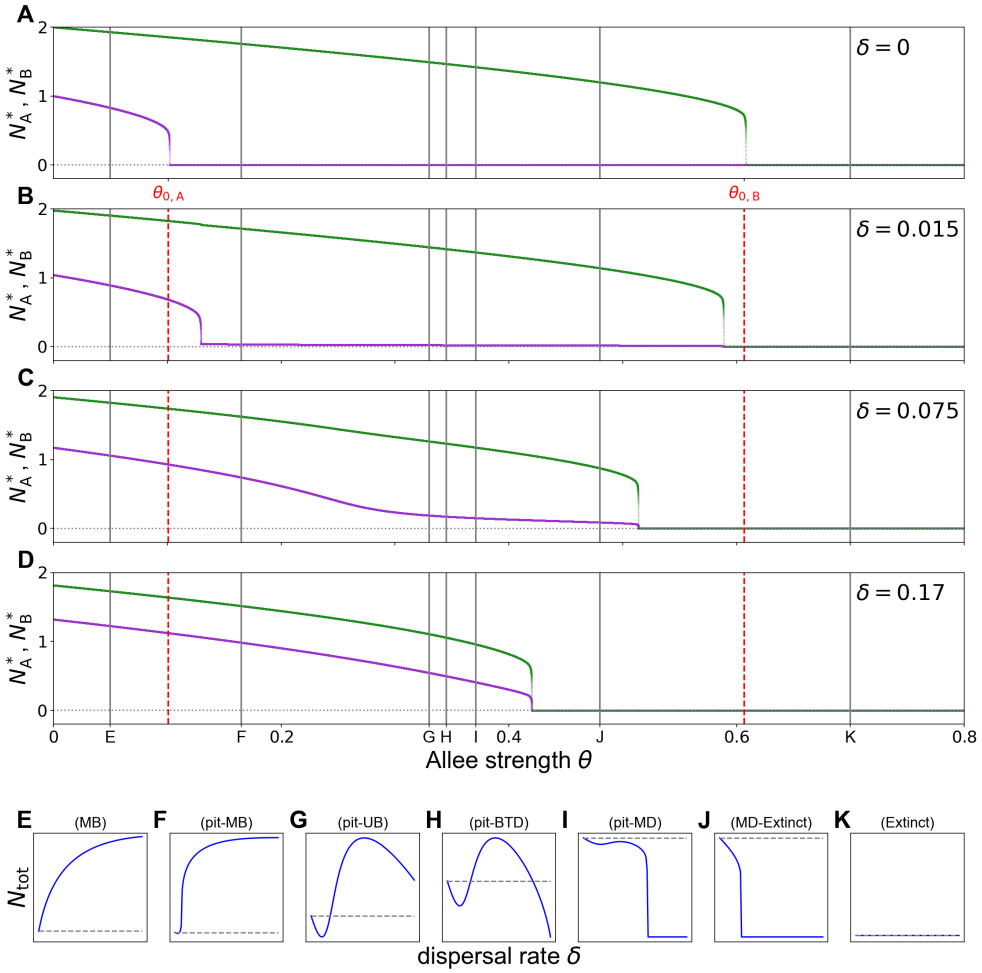

Fig. 3 The rescue effect and the Allee pit with their mechanisms. A–D: The diagrams show the asymptotic subpopulation sizes N_A^* and N_B^*, in purple and green respectively, for the initial condition $(1, 1)$ in terms of the Allee effect strength θ for different degrees of connectivity. The gray vertical lines indicate the θ–values which are chosen for the diagrams in the panels E–K. The dashed red vertical lines correspond to the critical Allee strength $\theta_{c,i}$. E–K: The asymptotic total population size is plotted in terms of the dispersal rate $\delta \in [0, 0.5]$. The dashed grey line is the reference value, i.e., the sum of the two carrying capacities. With varying θ, seven different (pit) response scenarios occur for this parameter setting, namely E: (MB) with $\theta = 0.05$, F: (pit–MB) with $\theta = 0.165$ having a rather small Allee pit which may be hard to see, G: (pit–UB) with $\theta = 0.33$, H: (pit–BTD) with $\theta = 0.345$, I: (pit–MD) with $\theta = 0.371$, J: (MD–Extinct) with $\theta = 0.48$, K: (Extinct) with $\theta = 0.7$. For all panels the parameters $r_A = 1.5$, $r_B = 3.5$, $K_A^{BH} = 1$ and $K_B^{BH} = 2$ are fixed.

The rescue effect induces new qualitative behaviors in the response scenarios. We found six so far unknown response scenarios. The major novelty is what we call an *Allee pit*. For small dispersal rates the asymptotic total population size falls below the sum of the two carrying capacities (our reference value) while for dispersal rates greater than a critical threshold (δ_{crit}) the asymptotic total population size can increase again beyond $K_{\text{A}} + K_{\text{B}}$. We refer to the new response scenarios which include an Allee pit as *pit response scenarios* (pit–MB, pit–UB, pit–BTD, and pit–MD) (shown in Fig. 3F–3I). They closely correspond to the four response scenarios MB, UB, BTD, and MD for $\theta = 0$, shown in Fig. 1. Moreover, a fifth and sixth new response scenario without an Allee pit were detected. One is closely related to the response scenario MD. Here the novelty is that for large dispersal rates the population goes extinct. In order to have a clear distinction, we call this new response scenario MD–Extinct (shown in Fig. 3J). Lastly, Extinct is the response scenario in which the population is extinct for all dispersal rates (shown in Fig. 3K). Generally in Fig. 3E–3K, we see how the response scenarios change with increasing Allee effect strength from the MB response scenario over pit response scenarios to the Extinct response scenario.

The Allee pit induces that the connectivity of the two patches needs to be above a critical value before the rescue effect can develop its beneficial impact on the asymptotic total population size. In the pit response scenarios (see Fig. 3F–3I and the referring vertical lines in Fig. 3A–3D), for very small dispersal rates the larger patch only loses individuals as the number of dispersing individuals is not high enough to push subpopulation A above its Allee threshold (vertical lines F, G, H and I in Fig. 3B). If subpopulation size A is below its Allee threshold, subpopulation A goes extinct and consequently there is no dispersal from patch A to patch B. Therefore, subpopulation B has only emigrants and no immigrants and a net loss results for the total population size. This is the reason for the Allee pit. Enhanced connectivity increases the number of dispersing individuals from B to A such that patch A can be rescued from extinction (follow the vertical lines F, G, H, and I to Fig. 3C and 3D). As soon as the rescue takes place, the total population size increases and can even increase beyond the reference value $K_{\text{A}} + K_{\text{B}}$ (in Figs. 3F, 3G, and 3H). The Allee pit is surpassed, and the total population benefits from the rescue effect. Larger dispersal rates can reduce the degree of benefit again or even cause drastic loss in population size and extinction. Therefore, it highly depends on the Allee strength θ whether it is beneficial or detrimental to increase the dispersal rate δ.

3.2 Impact of the Allee effect on the response scenarios

We now want to investigate how an increased Allee strength influences the resulting (pit) response scenarios. In particular, we aim to understand for which Allee strengths the Allee pit occurs, depending on habitat heterogeneity. Habitat heterogeneity can be represented by different values of the two carrying capacities K_{A} and K_{B}, and the two intrinsic growth rates r_{A} and r_{B}. Here, we fix K_{A}, K_{B} and r_{A} while varying r_{B} to obtain different degrees of heterogeneity. We therefore specifically investigate which parameter combinations of the Allee strength θ and habitat heterogeneity represented by r_{B} result in pit response scenarios. To explore this, we run numerical simulations for a large range of θ and r_{B} values. The parameter regions for pit response scenarios

lie in the so called 'rescue regions' as the rescue effect is the underlying mechanism of the pit response scenarios. We obtain two such rescue regions R_1 and R_2, in which one of the subpopulations rescues the other. Moreover, there is one region in which rescue is not necessary as both subpopulations survive independently (P); and one region where both subpopulations face total extinction (E). The results of our simulations are shown in Fig. 4. The four regions are indicated in the inset in Fig. 4. Each color indicates a distinct (pit) response scenario as indicated in the color bar. In order to illustrate how to understand this figure, we can look at Fig. 3E–3K which correspond to a horizontal cut through Fig. 4 for a fixed habitat heterogeneity, i.e., at $r_\mathrm{B} = 3.5$, along all the occurring (pit) response scenarios when the Allee strength is increased.

First, we are interested in the parameter regions for which the rescue effect occurs. For parameter combinations of θ and r_B for which only one of the two subpopulations persists in isolation, the rescue effect occurs as soon as the two patches are connected. Then, the rescue effect induces in many, but not all, cases an Allee pit. The *rescue regions* encompass all parameter combinations where either patch A is extinct in isolation and rescued by B, or vice versa. Therefore, the boundaries of the rescue regions are given by the critical Allee strengths $\theta_{\mathrm{c},i}$. The rescue effect occurs if and only if the Allee strength lies in between the two critical Allee strengths, i.e., for

$$\theta \in \begin{cases} (\theta_{\mathrm{c,A}}, \theta_{\mathrm{c,B}}), & \text{if } \theta_{\mathrm{c,A}} < \theta_{\mathrm{c,B}}, \\ (\theta_{\mathrm{c,B}}, \theta_{\mathrm{c,A}}), & \text{if } \theta_{\mathrm{c,B}} < \theta_{\mathrm{c,A}}, \end{cases}$$

where one subpopulation is extinct in isolation and the other subpopulation is viable.

In Figure 4 the boundaries are plotted based on Eq. (4), reformulated in terms of r_B. The dashed line indicates the critical Allee strength of patch A, which is independent of r_B (and therefore a vertical line). The dashdotted line indicates the critical Allee strength of patch B, which is dependent on r_B (and therefore a curve). As indicated in the inset in Fig. 4, these boundaries divide the diagram into the four regions:

- P – persistence of both patches,
- R_1 – rescue region,
- R_2 – inverse rescue region,
- E – extinction of both patches.

In addition to the two regions P and E, in this section we focus on the upper right rescue region R_1 in which the larger patch B rescues the smaller patch A. The rescue region R_2 in which the parameter values result in an *inverse rescue effect*, i.e., the smaller patch A rescues the larger patch B, is explained in Appendix B.

Region P encompasses parameter combinations for which patches A and B both persist in isolation and therefore the total population asymptotically persists. For $\theta = 0$, the parameter ranges for the four different response scenarios can be found analytically (Grumbach et al, 2023). For enhanced Allee strength ($\theta > 0$) the parameter region of the response scenario UB widens. The threshold value of r_B to the response scenario MB increases and the threshold value to the response scenarios BTD decreases. The parameter region of the response scenario MD shrinks. For Allee

strengths very close to $\theta_{c,A}$, also the parameter region of the response scenario BTD drastically shrinks, which may be hard to see in Fig. 4. Parameter combinations for which both subpopulations go extinct in isolation and therefore the entire population dies out, i.e., the response scenario Extinct, are part of region E.

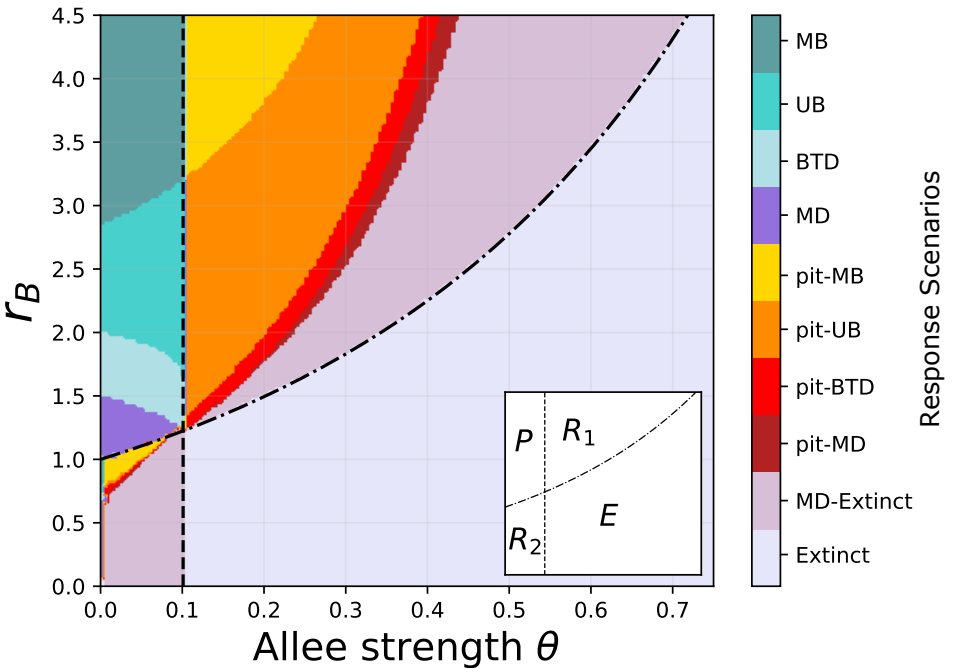

Fig. 4 The response scenarios for parameter combinations of the Allee strength θ and the growth rate r_B. Each color refers to one of the scenarios as indicated in the colorbar on the right side. The dashed and dashdotted lines coincide with the bifurcation points for the isolated subpopulations, i.e., $\theta_{0,A}$ and $\theta_{0,B}$, respectively, as given in Eq. (4). Schematically, the bifurcation curves are boundaries between the four regions P, R_1, R_2, and E as shown in the inset. The parameters $r_A = 1.5$, $K_A^{BH} = 1$ and $K_B^{BH} = 2$ are fixed. The method utilized to generate this figure is outlined in Appendix A.1. A zoom into the lower left corner, i.e., region R_2, can be found in Fig. A2 in Appendix A.

The rescue region R_1 encompasses the parameter region for which subpopulation A would be extinct in isolation. Connectivity can facilitate subpopulation B to rescue subpopulation A from extinction. The mechanism was explained in Sect. 3.1. The left boundary of R_1 is the critical Allee strength of patch A. This is the threshold at which the response scenarios without an Allee pit change to pit response scenarios. At this threshold MB switches to pit–MB, UB switches to pit–UB, and BTD switches to pit–BTD. The system changes from having five equilibria with three stable states to having three equilibia with only two stable states. The stable state which may disappear for

increased θ is the coexistence equilibrium $E_{\mathrm{Coex}} = (K_{\mathrm{A}}, K_{\mathrm{B}})$. Therefore, for small dispersal rates individuals from patch B move into patch A, where the subpopulation lies below its Allee threshold, which causes the Allee pit. Increased connectivity enables sufficiently many individuals to disperse into patch A such that the subpopulation size grows beyond the Allee threshold, the stable state E_{Coex} appears, and therefore both subpopulations coexist at a larger population size. This mechanism can be seen in the change of the existence of equilibria from Fig. 2E to 2F. For values of θ very close to the left boundary of R_1 the Allee pit is extremely narrow and shallow (cf. Fig. 5), i.e., connectivity 'immediately' (for an extremely small dispersal rate) rescues the extinct subpopulation.

At the right boundary of R_1 for Allee strengths below the critical value $\theta_{0,\mathrm{B}}$ the response scenario does not include an Allee pit. The conditions in both patches are highly vulnerable. The larger patch can avoid immediate extinction for small dispersal rates but cannot avoid extinction for greater dispersal rates. Therefore we obtain the MD–Extinct response scenario.

In the transition from P to R_1 and then to E, we discover that an increasing Allee strength increases the pressure on the total population. This pressure results in a change of response scenarios from beneficial ones to highly detrimental ones and even to extinction. A closer look at the width and depth of the Allee pit helps us to understand how the qualitatively similar response scenarios in one color segment of Fig. 4 differ in their potential consequences.

3.3 The width and depth of Allee pits

We already highlighted that the asymptotic total population size in isolation, i.e., $K_{\mathrm{A}} + K_{\mathrm{B}}$, decreases with increasing Allee strength θ. This pressure on the population might make a metapopulation even more prone to extinction. Especially the Allee pit can potentially further decrease a population size drastically close to zero or the Allee threshold such that small perturbations in external factors could drive a population to extinction. This risk of extinction can be diminished by increasing the dispersal rate beyond the critical dispersal rate δ_{crit} above which connectivity is beneficial. Therefore, we want to have a closer look at the width of Allee pits (which we define the distance between zero and the critical dispersal rate) and the depth of Allee pits (which we define the absolute difference between the sum of the two carrying capacities and the local minimum of the asymptotic total population size). We understand the depth of the Allee pit as a measure of the stochastic extinction probability.

The shapes of Allee pits vary a lot depending on the parameter values. They mainly differ in their width and depth as illustrated in Fig. 5. In Fig. 5A the pit is narrow and shallow which means the critical dispersal rate is very small and little risk comes along with the Allee pit. In contrast, in Fig. 5B the Allee pit is also very narrow but deep and therefore the population declines locally close to zero (or potentially to the Allee threshold). In Fig. 5C the Allee pit is very shallow but wide. The induced risk of stochastic extinction is rather low but the total population is less likely to benefit from increased connectivity. Figure 5D shows an Allee pit which is deep and wide. It induces a high risk of stochastic extinction which can only be diminished by drastically increasing connectivity.

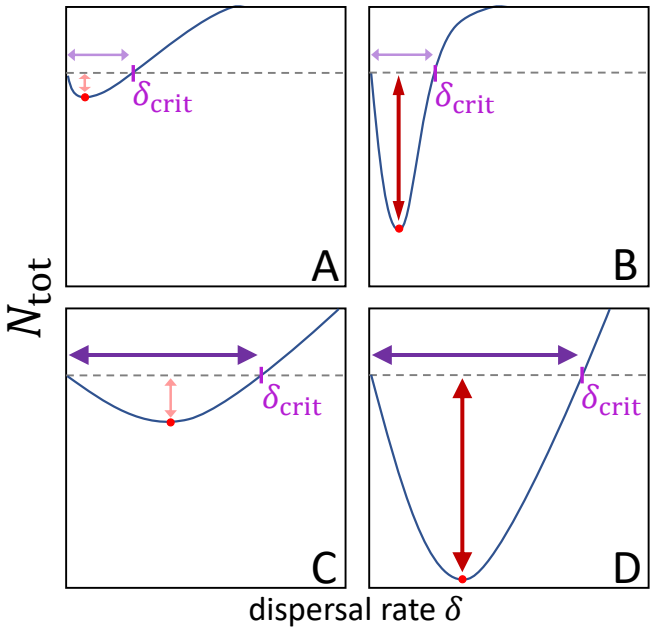

Fig. 5 Different shapes of Allee pits. They differ in width and depth and therefore in their critical dispersal rates δ_{crit} and risks of extinction (the distance from zero to the local minimum indicated by a red circle). The depth of the Allee pit varies in the four panels from shallow (left panels, indicated by thin and short red arrows) to deep (right panels, indicated by thick and long red arrows). The width of the Allee pit varies in the four panels from narrow (upper panels, indicated by thin and short purple arrows) to wide (lower panels, indicated by thick and long purple arrows).

Figure 6 shows the critical dispersal rate and the minimum asymptotic total population size of the Allee pits occuring in the pit response scenarios across a large range of parameter combinations of θ and r_{B}. The method utilized to generate this figure is outlined in Appendix A.2. Figure 6A focuses on the width of the Allee pit. The greater the Allee strength θ the larger the critical dispersal rate and therefore the wider the Allee pit. Within both rescue regions R_1 and R_2 (cf. Fig. 4), larger r_{B} values have a larger maximal width (indicated by a darker coloring) with increasing Allee strength.

In Figure 6B we see that for increased Allee strength θ the minimum population size decreases and therefore the Allee pit gets deeper. For parameter combinations close to the intersection of the region boundaries $\theta_{0,\text{A}}$ and $\theta_{0,\text{B}}$ the minimum takes lower values. Approaching the intersection, both patches get closer to their bifurcation points, i.e., close to extiction. This explains why the depth and width of the Allee pit increases (a lot) in a small neighborhood of the intersection. Especially for parameter combinations in R_2 the minimum is very close to zero, which induces an increased risk of extinction for the total population. We can infer that situations in which the smaller patch rescues the larger patch potentially generate a severe risk of extinction.

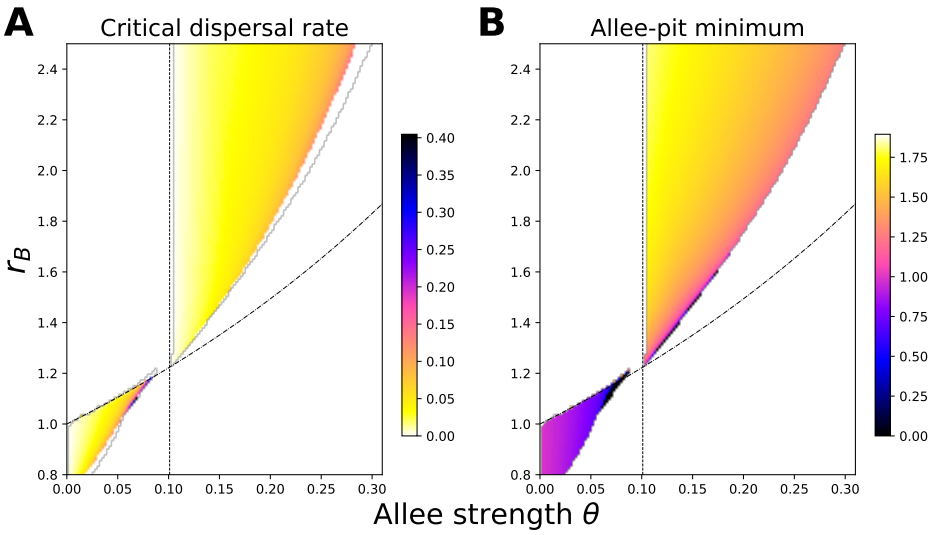

Fig. 6 Width and depth of Allee pits. A: The critical dispersal rate which corresponds to the width of the Allee pit. B: The minimum asymptotic total population size which corresponds to the depth of the Allee pit. The plots are generated only in parameter regions in which pit response scenarios occur; other parameter regions are shown in white. In both panels the dashed and dashdotted lines coincide with the boundaries $\theta_{0,\mathrm{A}}$ and $\theta_{0,\mathrm{B}}$ in Fig. 4. We fixed $r_{\mathrm{A}} = 1.5$, $K_{\mathrm{A}}^{\mathrm{BH}} = 1$ and $K_{\mathrm{B}}^{\mathrm{BH}} = 2$.

4 Discussion and Conclusions

We found that the mate-finding Allee effect in two connected patches can induce an Allee pit. The existence of the Allee pit signifies that mild or moderate increases in connectivity are detrimental, i.e. the asymptotic total population size decreases with increasing dispersal rate when the latter is low. This means that the Allee effect is another (and novel) mechanism where a stronger coupling between patches can be disadvantageous. The Allee pit can be 'dangerous' for a population as it may decrease the total population size drastically for certain degrees of connectivity. This is especially the case when the larger patch gets vulnerable and extinction prone (evident for parameter combinations in region R_2 in Fig. 6).

The difference between the pit response scenarios and other response scenarios is the Allee pit. It emerges from the 'attempt' of the larger patch to rescue the smaller one which results, for too little connectivity, in a loss of individuals for the total population. Individuals die after dispersing as the subpopulation size is still below the Allee threshold. That causes the Allee pit for small dispersal. Enhanced connectivity facilitates the occurrence of the rescue effect which can reestablish an extinct subpopulation, resulting in overcoming the Allee pit when a critical threshold of connectivity is surpassed. For dispersal rates beyond that critical dispersal rate the subpopulations grow above their Allee thresholds and total population then benefits from connectivity. The asymptotic total population size can increase beyond the sum of the two

carrying capacities and can thus turn from detrimental to beneficial. This could be an important point of orientation for conservation management, as the latter should increase connectivity to dispersal rates beyond those critical values. This would make sure that the connectivity is large enough to enable the population to gain from the rescue effect rather than suffering under the Allee pit risks. Apart from the Allee pit, the biological mechanisms behind the four pit response scenarios are qualitatively similar to the ones of the response scenarios MB, UB, BTD, and MD, respectively described in Grumbach et al (2023).

Two further response scenarios have been identified in this study: MD–Extinct and Extinct. In MD–Extinct, the asymptotic total population size decreases with increased connectivity, akin to MD, and goes extinct for large dispersal rates. This is because for some dispersal rates, one or both asymptotic subpopulation sizes fall below their Allee thresholds and therefore (sub-)population extinction occurs. If both subpopulation sizes remain above their Allee thresholds, the response scenario reverts to MD instead of MD–Extinct. This emphasizes once again that the Allee effect is particularly dangerous for small and declining populations. The Extinct response scenario only occurs when the Allee strength exceeds the critical Allee strengths of both subpopulations, resulting in extinction for both subpopulations in isolation as well as for all levels of connectivity.

Throughout this paper we looked at the rescue of one patch in which the subpopulation is extinct in isolation by another viable patch. Our framework can be biologically interpreted and applied in other contexts as well. The viable subpopulation can, for example, be understood as an invasive species which attempts to invade a new patch. In this setting the other subpopulation is zero, as the invasive species does not yet inhabit this patch. The Allee pit signifies a loss of individuals attempting to invade while for dispersal rates beyond the critical dispersal rate the invasive species can establish in the new patch.

It is interesting to look at circumstances under which Allee pits and the rescue effect occur. Figure 4 suggests that the range of Allee strengths θ inducing an Allee pit in region R_1 expands with r_B. Biological explanations for this might be that a larger growth rate in subpopulation B enables the subpopulation to reproduce faster. Therefore, it can rescue the other subpopulation A even for stronger Allee effects before the pressure of the Allee effect induces extinction. For other parameter settings we obtained a similar result.

Within the rescue region, the thresholds between the pit response scenarios were not described analytically here but obtained by numerical simulations. The explicit determination of these thresholds remains an open problem for future research. The analytical description of the critical dispersal rate remains an open question as well.

The coupled system which was investigated in this study can have up to nine equilibria, of which up to four are stable. For our numerical simulations we chose an inintial condition from the basin of attraction of the coexistence equilibrium $E_{\mathrm{Coex}} = (K_{\mathrm{A}}, K_{\mathrm{B}})$. In conservation ecology we are mostly interested in the highest chance of persistence for all subpopulations. As we saw in our results even the coexistence equilibrium E_{Coex} may be exposed to a high risk of extinction due to the Allee effect. With a different choice of initial conditions than the chosen one throughout this paper,

different stable equilibria would be approached. Given that the other equilibria are characterized by smaller (sub)population sizes, populations are at risk of extinction at lower Allee strength levels compared to the equilibrium E_{Coex}. While the results are expected to be comparable, other initial conditions could lead to narrower rescue regions and pits, potentially increasing the risk of stochastic extinction across a wider parameter range.

In this study the mate-finding Allee effect was considered. Among various forms of Allee effects, including those driven by predation or phenomenological factors, the mate-finding Allee effect stands out as one of the most frequently observed phenomena in empirical studies (Courchamp et al, 2008; Kramer et al, 2009). Results may be expected to hold qualitatively also for other forms of Allee effects, such as the predation-driven Allee effect. We assumed that the mate-finding Allee effect occurs symmetrically and independently within each patch. Nevertheless, it is an interesting question for future work to assume the Allee effect to occur in only one of the patches and how fragmentation complicates mate finding across (and not only within) different patches.

The term 'critical dispersal rate' has been used in various contexts in the literature and can refer to different phenomena. For instance, Vortkamp et al (2022) consider the BTD response scenario and define the critical dispersal rate as the smallest dispersal rate at which the asymptotic total population size falls below the reference value. Thus, their critical dispersal rate delineates a transition from a beneficial to a detrimental effect. Critical dispersal rates that mark a similar transition from positive to negative outcomes, e.g., from survival to extinction, have been found when dispersal is costly (Kirkland et al, 2006) or from suitable habitats to hostile environments as in the KiSS model (Kierstead and Slobodkin, 1953; Skellam, 1951), see Ryabov and Blasius (2008) for a review. By contrast, our critical dispersal rate describes a transition from negative to positive effects of increasing dispersal, as it identifies the dispersal rate at which the detrimental Allee pit switches to a beneficial effect. Similar positive effects of increased dispersal have been observed in patch occupancy models when a metapopulation is to balance local extinction by recolonization (Levins, 1969) or in spatially explicit models when a single population is to track shifting climatic conditions (Potapov and Lewis, 2004; Leroux et al, 2013; Kerr, 2020), prevent being washed out in advective environments such as streams and rivers (Speirs and Gurney, 2001; Lutscher et al, 2005; Hilker and Lewis, 2010), or avoid sinking in the vertical water column (Shigesada and Okubo, 1981; Huisman et al, 2002). Vortkamp et al (2020) found that dispersal can prevent essential extinction in coupled patches with Allee thresholds and overcompensation.

In the context of conservation and landscape planning, the question of which management strategies are the most effective often centers on identifying and promoting optimal network structures (e.g., Watts et al, 2009; DeAngelis et al, 2021). However, 'optimal' can be understood in various ways: in terms of maximizing biomass (e.g., Gadgil, 1971; Freedman and Waltman, 1977; DeAngelis et al, 1979; Vance, 1980; Holt, 1985; Arditi et al, 2015; Franco and Ruiz-Herrera, 2015; Zhang et al, 2017; Grumbach et al, 2023), enhancing growth rates (e.g., Nguyen et al, 2023), ensuring evolutionary stability (e.g., Kirkland et al, 2006), or determining the ideal spacing between habitat

patches in presence of disturbances (e.g., White et al, 2021; Crespo-Miguel et al, 2022). The work of White et al (2021) emphasizes the trade-off between disturbance impacts and successful dispersal for recolonization, concluding that intermediate patch spacing (translating into intermediate dispersal) is optimal. Also in our results there are scenarios in which intermediate dispersal rates maximize the asymptotic total population size, namely BTD and pit–BTD. But the crucial point in our findings is the existence of a *critical* dispersal rate; if not exceeded, small increases in dispersal can lead to worse outcomes rather than improvements, suggesting that no management is better than poor management. The critical dispersal rate emerges solely through spatial heterogeneity and the Allee effect, even in the absence of disturbances and distance-dependent dispersal success. This underlines the importance of considering life-history trade-offs in the context of Allee effects, which can play a crucial role in determining the best management strategies, where avoiding worsening the situation could be more critical than finding the optimal solution.

In summary, our study underlines the pivotal role of connectivity and the Allee effect in shaping population dynamics in fragmented habitats. We found that low connectivity can lead to population declines in form of Allee pits, while enhanced connectivity facilitates the rescue effect, mitigating extinction risks. Our results emphasize the importance of achieving dispersal rates above a critical threshold to maximize the benefits of connectivity for population persistence. Overall, these findings offer fundamental and potentially valuable insights for the development of effective conservation strategies in fragmented landscapes.

Statements and Declarations

Acknowledgements

The authors gratefully acknowledge discussions with Irina Vortkamp, Femke Reurik, Daniel Franco, and Juan Segura. CG expresses her gratitude to Atsushi Yamauchi, Hiromi Seno, Jia–Yuan Dai, Sze–Bi Hsu, and Shih–Bin Wang for insightful discussions during CG's research stay in Japan and Taiwan, to the members of Meike Wittmann's lab meeting and the members of the Institute of Marine Affairs and Resource Management at the National Taiwan Ocean University for valuable input, and to Christian Guill and Bernd Blasius for fruitful exchanges.

Funding

This research was partially supported by the German Academic Exchange Service (DAAD) with funds from the Federal Foreign Office, and by the Universitätsgesellschaft Osnabrück.

Competing Interests

The authors have no relevant financial or non-financial interests to disclose.

Author Contributions

Formal analysis and investigation of the results: CG; Methodology: all authors; Conceptualization and supervision: FMH; Writing – original draft preparation: CG; Writing – Review and editing: all authors.

ORCID numbers

Carolin Grumbach: 0000-0001-9332-1388
Frank M. Hilker: 0000-0001-5470-8889

Appendix A Numerical methods

A.1 Methods for Figure 4

In the following we explain the numerical method which we utilized to generate Fig. 4. We solved Eq. (1) with the initial condition $(1, 1)$, which lies in the basin of attraction of the equilibrium (K_A, K_B) if it exists, for 500 time steps. We repeated this for 300 equidistant dispersal rates $\delta \in [0, 0.5]$. We also did this for a large range of Allee strengths and growth rates in patch B, each with 180 equidistant values in the ranges shown in Fig 4. All other parameter values were fixed.

For each parameter combination of θ and r_B, and for each dispersal rate value, we saved the total population size, i.e., the sum of N_A^* and N_B^* in Eq. (1), after 500 time steps. We interpreted the total population size at the 500^{th} time step as the asymptotic total population size N_{tot}, to which we refer as the ATPS. We did not find any evidence for sustained oscillations.

As the respective reference value Ref for the ATPS, marking the transition between beneficial and detrimental effects, we used the ATPS at $\delta = 0$, i.e., $K_A + K_B$. For each combination of θ and r_B, let ATPS(δ) denote the ATPS for one of the discretized dispersal rate values. ATPS($\delta_{\max}$) is the ATPS at the largest dispersal rate value. Then ATPS($\Delta\delta$) is the ATPS at the smallest positive dispersal rate value, as $\Delta\delta$ is the step size of the dispersal rate discretization. The response scenarios for each parameter combination of θ and r_B were detected and classified by four different criteria as visualized in Fig. A1.

The first step of the classification is based on the slope of the ATPS at zero dispersal (cf. Fig. A1(I)). To this end, we compared the ATPS at the smallest positive dispersal rate to Ref. The ATPS($\Delta\delta$) lies above Ref for the response scenarios MB, UB, and BTD. The ATPS($\Delta\delta$) is equal to Ref in the response scenario Extinct; in this case, the ATPS is zero for all dispersal rates. The ATPS($\Delta\delta$) lies below Ref for all pit response scenarios and the detrimental response scenarios (MD, MD–Extinct).

Second, we distinguished the two resulting groups of response scenarios by comparing the ATPS at the largest dispersal rate value, i.e., ATPS($\delta_{\max}$), to Ref (cf. Fig. A1(II)). The response scenarios which have a beneficial effect for large dispersal rates are MB and UB with a positive slope in (I), and pit–MB and pit–UB with a negative slope in (I). The response scenarios which have a detrimental effect or lead to extinction for large dispersal rates are BTD with a positive slope in (I), and pit–BTD, pit–MD, MD, and MD–Extinct with a negative slope in (I).

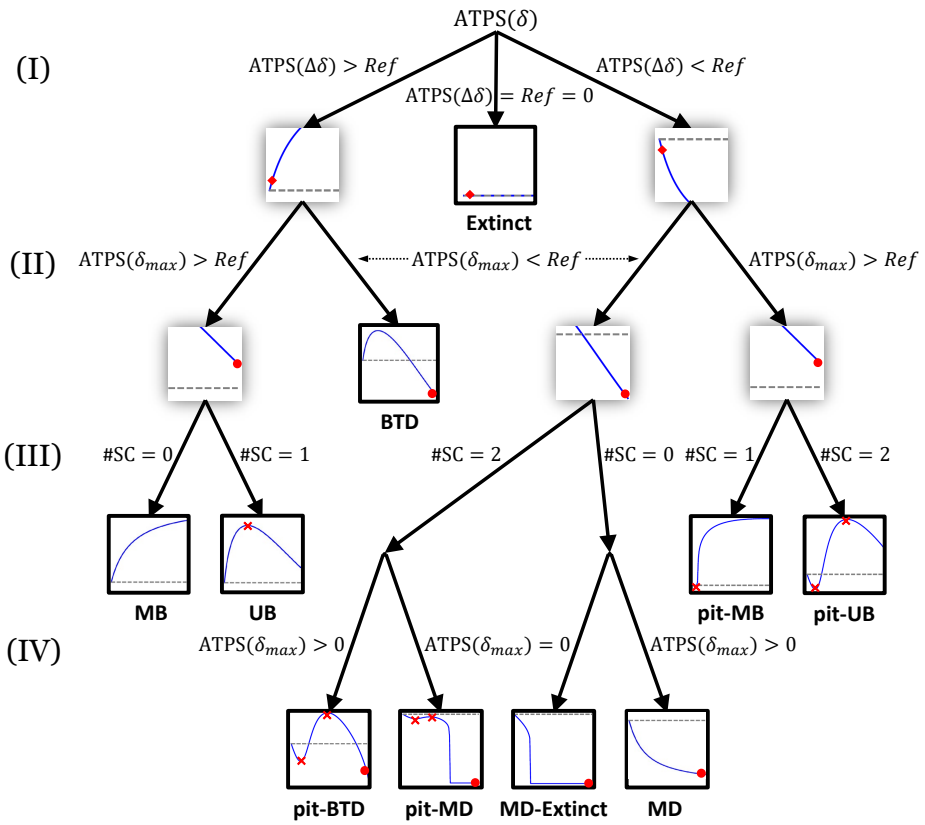

Fig. A1 The decision tree for the classification of the response scenarios. ATPS($\Delta\delta$) is the asymptotic total population size at the smallest positive dispersal rate. ATPS($\delta_{\max}$) is the asymptotic total population size at the largest dispersal rate value. #SC is the count of the sign changes of the differences between the ATPS at consecutive dispersal rate values. The red symbols indicate the criteria (I)–(IV) in the small graphs, which sketch the ATPS as a function of the dispersal rate.

Third, we further distinguished the response scenarios based on the number of local extrema of ATPS(δ). Therefore, we counted the number of changes in the slope of the ATPS, which we calculated by comparing the signs of the differences between ATPSs at consecutive dispersal rate values δ_i and δ_{i+1}, where $i \in [0, 299]$ (cf. Fig. A1(III)). This served to clearly distinguish between the response scenarios MB (zero extrema), UB (one maximum), pit–MB (one minimum), and pit–UB (two extrema). This leaves pit–BTD and pit–MD (each of which have two local extrema), and MD–Extinct and MD (each of which have no local extrema), for which we used a further criterion.

Finally, by checking whether the ATPS at the largest dispersal rate value, i.e., ATPS($\delta_{\max}$), is positive or zero, we distinguished between pit–BTD (positive at largest dispersal rate), pit–MD (zero at largest dispersal rate), MD (positive at largest dispersal rate), and MD–Extinct (zero at largest dispersal rate) (cf. Fig. A1(IV)).

A.2 Methods for Figure 6

In the following we explain the numerical method which we utilized to generate Fig. 6. To calculate the critical dispersal rate and the minimum ATPS for the four pit response scenarios, we used the response scenario classification outlined in Appendix A.1.

As the critical dispersal rate we saved the dispersal rate value for which the difference between the ATPS and Ref (which is negative for small dispersal rates due to the Allee pit) is either zero or positive for the first time when increasing the discretized dispersal rate.

In order to determine the Allee pit minimum, we looked for the first change from a negative to a positive slope of the ATPS when increasing the discretized dispersal rate. We started from dispersal rate zero. As the minimum we saved the ATPS for the dispersal rate value for which the difference between two consecutive ATPSs is either zero or positive for the first time.

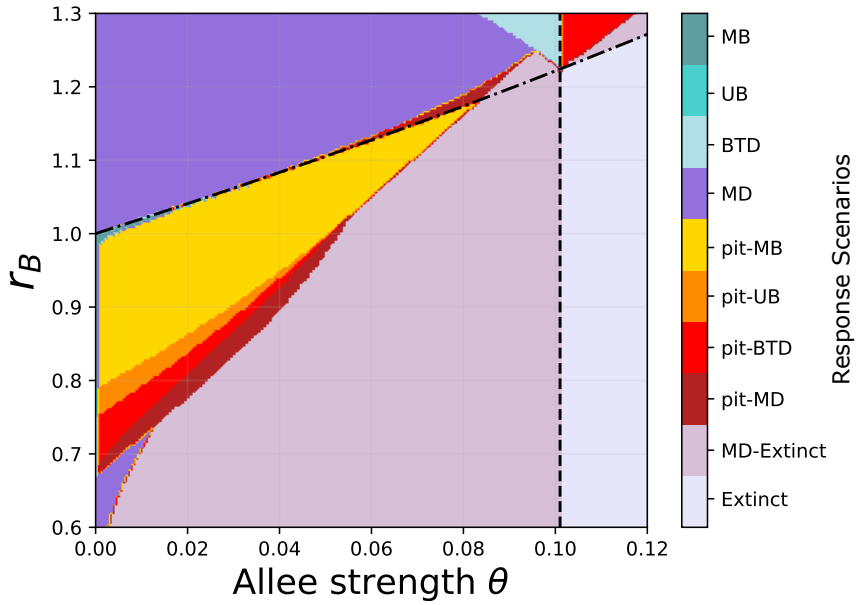

Fig. A2 The response scenarios in rescue region R_2, i.e., the inverse rescue effect, for parameter combinations of the Allee strength θ and the growth rate r_B. This is a zoom into the lower left corner of Fig. 4. Each color refers to one of the response scenarios as indicated in the colorbar. The dashed and dashdotted lines coincide with the boundaries in the inset of Fig. 4. The parameters $r_A = 1.5$, $K_A^{BH} = 1$ and $K_B^{BH} = 2$ are fixed.

Appendix B The inverse rescue effect

In Sect. 3.2 we closely looked at the change of the response scenarios for increasing Allee strength. We focused on the rescue region R_1 in Fig. 4, in which the larger subpopulation B persists in isolation, while the smaller subpopulation A would die out in isolation. Therefore, in R_1 patch B rescues patch A. Here, we briefly look at region R_2 in which the *inverse rescue effect* occurs, i.e., 'the smaller' (in terms of K_i^{BH}) subpopulation A survives in isolation and can rescue 'the larger' subpopulation B by increased connectivity.

Figure A2 shows the results of our numerical simulations zoomed in the parameter values of region R_2. In the absence of the Allee effect only the four response scenarios MB, UB, BTD, and MD occur. As soon as the Allee strength is greater than zero, we obtain the pit response scenarios due to the rescue effect in the rescue region R_2. For smaller r_2–values we still obtain the MD response scenario for small Allee strengths. For increased Allee strength the parameter combinations in rescue region R_2 result in the MD–Extinct response scenario. Patch A can prevent patch B from immediate extinction for small dispersal but for larger dispersal the total population dies out.

References

Amarasekare P (1998) Interactions between local dynamics and dispersal: insights from single species models. Theoretical Population Biology 53(1):44–59. https://doi.org/10.1006/tpbi.1997.1340

Arditi R, Lobry C, Sari T (2015) Is dispersal always beneficial to carrying capacity? New insights from the multi-patch logistic equation. Theoretical Population Biology 106:45–59. https://doi.org/10.1016/j.tpb.2015.10.001

Boukal DS, Berec L (2009) Modelling mate-finding Allee effects and populations dynamics, with applications in pest control. Population Ecology 51:445–458. https://doi.org/10.1007/s10144-009-0154-4

Brown JH, Kodric-Brown A (1977) Turnover rates in insular biogeography: effect of immigration on extinction. Ecology 58(2):445–449. https://doi.org/10.2307/1935620

Chen L, Liu T, Chen F (2022) Stability and bifurcation in a two-patch model with additive Allee effect. AIMS Mathematics 7(1):536–551. https://doi.org/10.3934/math.2022034

Courchamp F, Clutton-Brock T, Grenfell B (1999) Inverse density dependence and the Allee effect. Trends in Ecology & Evolution 14(10):405–410. https://doi.org/10.1016/S0169-5347(99)01683-3

Courchamp F, Berec L, Gascoigne J (2008) Allee Effects in Ecology and Conservation. Oxford University Press, Oxford, https://doi.org/10.1093/acprof:oso/9780198570301.001.0001

Crespo-Miguel R, Jarillo J, Cao-García FJ (2022) Scaling of population resilience with dispersal length and habitat size. Journal of Statistical Mechanics: Theory and Experiment 2022(2):023,501. https://doi.org/10.1088/1742-5468/ac4982

Cronin JT, Fonseka N, Goddard J, et al (2020) Modeling the effects of density dependent emigration, weak Allee effects, and matrix hostility on patch-level population persistence. Mathematical Biosciences and Engineering 17(2):1718. https://doi.org/10.3934/mbe.2020090

DeAngelis D, Travis C, Post W (1979) Persistence and stability of seed-dispersed species in a patchy environment. Theoretical Population Biology 16(2):107–125. https://doi.org/10.1016/0040-5809(79)90008-X

DeAngelis D, Zhang B, Ni WM, et al (2020) Carrying capacity of a population diffusing in a heterogeneous environment. Mathematics 8(1):49. https://doi.org/10.3390/math8010049

DeAngelis DL, Zhang B (2014) Effects of dispersal in a non-uniform environment on population dynamics and competition: A patch model approach. Discrete & Continuous Dynamical Systems - B 19(10):3087–3104. https://doi.org/10.3934/dcdsb.2014.19.3087

DeAngelis DL, Franco D, Hastings A, et al (2021) Towards building a sustainable future: positioning ecological modelling for impact in ecosystems management. Bulletin of Mathematical Biology 83:1–28. https://doi.org/10.1007/s11538-021-00927-y

Dennis B (1989) Allee effects: population growth, critical density, and the chance of extinction. Natural Resource Modeling 3(4):481–538

Fahrig L (2002) Effect of habitat fragmentation on the extinction threshold: a synthesis. Ecological Applications 12(2):346–353. https://doi.org/10.1890/1051-0761(2002)012[0346:EOHFOT]2.0.CO;2

Fahrig L (2017) Ecological responses to habitat fragmentation per se. Annual Review of Ecology, Evolution, and Systematics 48:1–23. https://doi.org/10.1146/annurev-ecolsys-110316-022612

Fahrig L, Arroyo-Rodríguez V, Bennett JR, et al (2019) Is habitat fragmentation bad for biodiversity? Biological Conservation 230:179–186. https://doi.org/10.1016/j.biocon.2018.12.026

Ferdy JB, Molofsky J (2002) Allee effect, spatial structure and species coexistence. Journal of Theoretical Biology 217(4):413–424. https://doi.org/10.1006/jtbi.2002.3051

Fletcher Jr RJ, Didham RK, Banks-Leite C, et al (2018) Is habitat fragmentation good for biodiversity? Biological Conservation 226:9–15. https://doi.org/10.1016/j.

738 biocon.2018.07.022

739 Franco D, Ruiz-Herrera A (2015) To connect or not to connect isolated patches.
740 Journal of Theoretical Biology 370:72–80. https://doi.org/10.1016/j.jtbi.2015.01.
741 029

742 Freedman H, Waltman P (1977) Mathematical models of population interactions with
743 dispersal. I: Stability of two habitats with and without a predator. SIAM Journal
744 on Applied Mathematics 32(3):631–648. https://doi.org/10.1137/0132052

745 Gadgil M (1971) Dispersal: population consequences and evolution. Ecology 52(2):253–
746 261. https://doi.org/10.2307/1934583

747 Gao D, Lou Y (2022) Total biomass of a single population in two-patch environments.
748 Theoretical Population Biology 146:1–14. https://doi.org/10.1016/j.tpb.2022.05.003

749 Gascoigne J, Berec L, Gregory S, et al (2009) Dangerously few liaisons: a review of
750 mate-finding Allee effects. Population Ecology 51:355–372. https://doi.org/10.1007/
751 s10144-009-0146-4

752 Gotelli NJ (1991) Metapopulation models: the rescue effect, the propagule rain, and
753 the core-satellite hypothesis. The American Naturalist 138(3):768–776. https://doi.
754 org/10.1086/285249

755 Grumbach C, Reurik FN, Segura J, et al (2023) The effect of dispersal on asymptotic
756 total population size in discrete-and continuous-time two-patch models. Journal of
757 Mathematical Biology 87(4):60. https://doi.org/10.1007/s00285-023-01984-8

758 Gyllenberg M, Hemminki J, Tammaru T (1999) Allee effects can both conserve and
759 create spatial heterogeneity in population densities. Theoretical Population Biology
760 56(3):231–242. https://doi.org/10.1006/tpbi.1999.1430

761 Haddad NM, Brudvig LA, Damschen EI, et al (2014) Potential negative ecological
762 effects of corridors. Conservation Biology 28(5):1178–1187. https://doi.org/10.1111/
763 cobi.12323

764 Hilker FM, Lewis MA (2010) Predator–prey systems in streams and rivers. Theoretical
765 Ecology 3:175–193. https://doi.org/10.1007/s12080-009-0062-4

766 Holt RD (1985) Population dynamics in two-patch environments: some anomalous
767 consequences of an optimal habitat distribution. Theoretical Population Biology
768 28(2):181–208. https://doi.org/10.1016/0040-5809(85)90027-9

769 Huisman J, Arrayás M, Ebert U, et al (2002) How do sinking phytoplankton species
770 manage to persist? The American Naturalist 159(3):245–254. https://doi.org/10.
771 1086/338511

IPBES (2019) Summary for policymakers of the global assessment report on biodiversity and ecosystem services of the Intergovernmental Science-Policy Platform on Biodiversity and Ecosystem Services. IPBES secretariat, Bonn, Germany, https://doi.org/10.5281/zenodo.3831673

Kang Y (2013) Scramble competitions can rescue endangered species subject to strong Allee effects. Mathematical Biosciences 241(1):75–87. https://doi.org/10.1016/j.mbs.2012.09.002

Kang Y (2015) Dynamics of a generalized Beverton-Holt competition model subject to allee effects. arXiv preprint arXiv:150505913 https://doi.org/10.48550/arXiv.1505.05913

Kang Y, Armbruster D (2011) Dispersal effects on a discrete two-patch model for plant–insect interactions. Journal of Theoretical Biology 268(1):84–97. https://doi.org/10.1016/j.jtbi.2010.09.033

Kerr JT (2020) Racing against change: understanding dispersal and persistence to improve species' conservation prospects. Proceedings of the Royal Society B 287(1939):20202,061. https://doi.org/10.1098/rspb.2020.2061

Kierstead H, Slobodkin LB (1953) The size of water masses containing plankton blooms. Journal of Marine Research 12(1):141–147

Kirkland S, Li CK, Schreiber SJ (2006) On the evolution of dispersal in patchy landscapes. SIAM Journal on Applied Mathematics 66(4):1366–1382. https://doi.org/10.1137/050628933

Kramer AM, Dennis B, Liebhold AM, et al (2009) The evidence for Allee effects. Population Ecology 51:341–354. https://doi.org/10.1007/s10144-009-0152-6

Leroux SJ, Larrivée M, Boucher-Lalonde V, et al (2013) Mechanistic models for the spatial spread of species under climate change. Ecological Applications 23(4):815–828. https://doi.org/10.1890/12-1407.1

Levins R (1969) Some demographic and genetic consequences of environmental heterogeneity for biological control. Bulletin of the Entomological Society of America 15(3):237–240. https://doi.org/10.1093/besa/15.3.237

Lutscher F, Pachepsky E, Lewis MA (2005) The effect of dispersal patterns on stream populations. SIAM Review 47(4):749–772. https://doi.org/10.1137/05063615

Maciel GA, Lutscher F (2015) Allee effects and population spread in patchy landscapes. Journal of Biological Dynamics 9(1):109–123. https://doi.org/10.1080/17513758.2015.1027309

Matter SF (2001) Synchrony, extinction, and dynamics of spatially segregated, heterogeneous populations. Ecological Modelling 141(1-3):217–226. https://doi.org/10.1016/S0304-3800(01)00275-7

Miller-Rushing AJ, Primack RB, Devictor V, et al (2019) How does habitat fragmentation affect biodiversity? A controversial question at the core of conservation biology. Biological Conservation 232:271–273. https://doi.org/10.1016/j.biocon.2018.12.029

Nguyen TD, Wu Y, Veprauskas A, et al (2023) Maximizing metapopulation growth rate and biomass in stream networks. SIAM Journal on Applied Mathematics 83(6):2145–2168. https://doi.org/10.1137/23M1556757

Pal D, Samanta G (2018) Effects of dispersal speed and strong Allee effect on stability of a two-patch predator–prey model. International Journal of Dynamics and Control 6:1484–1495. https://doi.org/10.1007/s40435-018-0407-1

Potapov AB, Lewis MA (2004) Climate and competition: The effect of moving range boundaries on habitat invasibility. Bulletin of Mathematical Biology 66:975–1008. https://doi.org/10.1016/j.bulm.2003.10.010

Ryabov AB, Blasius B (2008) Population growth and persistence in a heterogeneous environment: the role of diffusion and advection. Mathematical Modelling of Natural Phenomena 3(3):42–86. https://doi.org/10.1051/mmnp:2008064

Saha S, Samanta G (2019) Influence of dispersal and strong Allee effect on a two-patch predator–prey model. International Journal of Dynamics and Control 7:1321–1349. https://doi.org/10.1007/s40435-018-0490-3

Sato K (2009) Allee threshold and extinction threshold for spatially explicit metapopulation dynamics with Allee effects. Population Ecology 51:411–418. https://doi.org/10.1007/s10144-009-0156-2

Schreiber SJ (2003) Allee effects, extinctions, and chaotic transients in simple population models. Theoretical Population Biology 64(2):201–209. https://doi.org/10.1016/S0040-5809(03)00072-8

Shigesada N, Okubo A (1981) Analysis of the self-shading effect on algal vertical distribution in natural waters. Journal of Mathematical Biology 12:311–326. https://doi.org/10.1007/BF00276919

Simberloff D, Cox J (1987) Consequences and costs of conservation corridors. Conservation Biology 1(1):63–71. https://doi.org/10.1111/j.1523-1739.1987.tb00010.x

Skellam JG (1951) Random dispersal in theoretical populations. Biometrika 38(1/2):196–218. https://doi.org/10.2307/2332328

Soanes K, Rytwinski T, Fahrig L, et al (2024) Do wildlife crossing structures mitigate the barrier effect of roads on animal movement? A global assessment. Journal of Applied Ecology 61(3):417–430. https://doi.org/10.1111/1365-2664.14582

Speirs DC, Gurney WSC (2001) Population persistence in rivers and estuaries. Ecology 82(5):1219–1237. https://doi.org/10.1890/0012-9658(2001)082[1219:PPIRAE]2.0.CO;2

Sun GQ (2016) Mathematical modeling of population dynamics with Allee effect. Nonlinear Dynamics 85:1–12. https://doi.org/10.1007/s11071-016-2671-y

Tewksbury JJ, Levey DJ, Haddad NM, et al (2002) Corridors affect plants, animals, and their interactions in fragmented landscapes. Proceedings of the National Academy of Sciences 99(20):12,923–12,926. https://doi.org/10.1073/pnas.202242699

Turner MG, Gardner RH, O'neill RV, et al (2001) Landscape ecology in theory and practice. Springer New York, https://doi.org/10.1007/b97434

Van Schmidt ND, Beissinger SR (2020) The rescue effect and inference from isolation–extinction relationships. Ecology Letters 23(4):598–606. https://doi.org/10.1111/ele.13460

Vance RR (1980) The effect of dispersal on population size in a temporally varying environment. Theoretical Population Biology 18(3):343–362. https://doi.org/0.1016/0040-5809(80)90058-1

Vortkamp I, Schreiber SJ, Hastings A, et al (2020) Multiple attractors and long transients in spatially structured populations with an allee effect. Bulletin of Mathematical Biology 82:1–21. https://doi.org/10.1007/s11538-020-00750-x

Vortkamp I, Kost C, Hermann M, et al (2022) Dispersal between interconnected patches can reduce the total population size. bioRxiv 2022.04.28.489935. https://doi.org/10.1101/2022.04.28.489935

Wang W (2016) Population dispersal and Allee effect. Ricerche di Matematica 65(2):535–548. https://doi.org/10.1007/s11587-016-0273-0

Watts ME, Ball IR, Stewart RS, et al (2009) Marxan with zones: Software for optimal conservation based land-and sea-use zoning. Environmental Modelling & Software 24(12):1513–1521. https://doi.org/10.1016/j.envsoft.2009.06.005

White ER, Baskett ML, Hastings A (2021) Catastrophes, connectivity and allee effects in the design of marine reserve networks. Oikos 130(3):366–376. https://doi.org/10.1111/oik.07770

874 Zhang B, Kula A, Mack KM, et al (2017) Carrying capacity in a heterogeneous
875 environment with habitat connectivity. Ecology letters 20(9):1118–1128